J Arid Land (2023) 15(2): 180–190
https://doi.org/10.1007/s40333-023-0005-8

Science Press Springer-Verlag

Sediment yield and erosion–deposition distribution characteristics in ephemeral gullies in black soil areas under geocell protection

WANG Xinyu[1], SU Yu[1], SUN Yiqiu[1], ZHANG Yan[2], GUAN Yinghui[2], WANG Zhirong[1], WU Hailong[1*]

[1] School of Environmental Science and Safety Engineering, Tianjin University of Technology, Tianjin 300384, China;
[2] School of Soil and Water Conservation, Beijing Forestry University, Beijing 100038, China

Abstract: Investigating the effect of geocells on the erosion and deposition distribution of ephemeral gullies in the black soil area of Northeast China can provide a scientific basis for the allocation of soil and water conservation measures in ephemeral gullies. In this study, an artificial simulated confluence test and stereoscopic photogrammetry were used to analyze the distribution characteristics of erosion and deposition in ephemeral gullies protected by geocells and the effect of different confluence flows on the erosion process of ephemeral gullies. Results showed that when the confluence flow was larger, the effect of geocell was more evident, and the protection against ephemeral gully erosion was stronger. When the confluence flow rates were 0.6, 1.8, 2.4, and 3.0 m^3/h, ephemeral gully erosion decreased by 37.84%, 26.09%, 21.40%, and 35.45%. When the confluence flow rates were 2.4 and 3.0 m^3/h, the average sediment yield rate of the ephemeral gully was close to 2.14 kg/(m^2·min), and the protective effect of ephemeral gully erosion was enhanced. When the flow rate was higher, the surface fracture of the ephemeral gully was more serious. With an increase in confluence flow rate, the ratio of erosion to deposition increased gradually, the erosion area of ephemeral gullies was expanded, and erosion depth changed minimally. In conclusion, geocell measures changed erosion patterns by altering the rill erosion/deposition ratio, converting erosion from rill erosion to sheet erosion.

Keywords: geocell; erosion and deposition distribution; runoff and sediment production; ephemeral gully; soil conservation

Citation: WANG Xinyu, SU Yu, SUN Yiqiu, ZHANG Yan, GUAN Yinghui, WANG Zhirong, WU Hailong. 2023. Sediment yield and erosion–deposition distribution characteristics in ephemeral gullies in black soil areas under geocell protection. Journal of Arid Land, 15(2): 180–190. https://doi.org/10.1007/s40333-023-0005-8

1 Introduction

Ephemeral gullies are developed by the continuous intensified erosion of rills. The major causes of ephemeral gully erosion are microtopographic fluctuations and unreasonable farming methods, and the long-term existence of ephemeral gully will accelerate soil erosion and change the surface slope (Liu et al., 2013; Douglas-Mankin et al., 2020; Xu et al., 2022). Statistics show that the existing area of soil erosion in the black soil of China is 27.59 km^2, accounting for about 27% of the total black soil area, while the number of erosion ditches produced by hydraulic erosion is about 29×10^4 (MWR (Ministry of Water Resources), 2013). Generally, the control of erosion

*Corresponding author: WU Hailong (E-mail: wuhailong@email.tjut.edu.cn)
Received 2022-07-23; revised 2022-12-15; accepted 2023-01-13

gullies on the slope of black soil involves the engineering measures of large ditches such as gullies (Liu et al., 2019). For an ephemeral gully with an average width smaller than 1.0 m and a depth of less than 0.5 m, adopting engineering measures, such as check dam and drop, is unsuitable (Nouwakpo and Huang, 2012). Herbaceous vegetation cover and buffer strip with bund can effectively control water and soil loss in an ephemeral gully, improve soil erosion resistance and corrosion resistance, and exert a significant effect on soil consolidation and water retention (Tang et al., 2012; Xiao et al., 2021; Ma et al., 2022). However, compared with other soil erosion areas in China, ephemeral gully erosion in the black soil area is more intense due to the "gully effect" and more runoff produced by long gentle slopes (Meng and Li, 2009). Concentrated runoff from a single rainfall event during the early stages of grass growth can wash away grass, reducing vegetation coverage and affecting the effectiveness of revegetation in ephemeral gullies. Therefore, improving the vegetation coverage of erosion ditches is particularly important to control the runoff scour of ephemeral gullies.

Geocells not only reinforce the slope to reduce water erosion but also prevent grass seeds and seedlings from being washed away by runoff, improving grass coverage (Sutherland, 1998). Geocells are also widely used in foundation reinforcement, scour protection, and road extension because of their good drainage, lateral restraint properties, and ease of transport (Banerjee et al., 2020). Yan et al. (2005) found that geocells can improve the erosion resistance of slopes by 40%; when time is longer, the effect is more evident. Geocells also exert considerable inhibitory effect on gully formation. Wang et al. (2012) explored the effects of slope and catchment flow on the scour resistance of geocell slopes and found that geocell-protected slopes generally do not form continuous scour gully. Water will flow along the edge of the geocell, extending the flow path of the slope flow and reducing the flow energy of water. Zeng et al. (2017) also found that geocells exhibit certain energy-dissipating and energy-impeding effects on water flow, and soil is spatially protected by geocells and less likely to form gully erosion. The aforementioned studies have shown that geocells can reduce erosion and inhibit gully erosion at different slopes, catchment flows, and rainfall intensities. However, quantitative data and the exploration of the evolution of soil erosion–deposition under geocell protection and the application of geocell to the management of ephemeral gullies are still lacking.

Stereophotogrammetry is a 3D model reconstruction technology characterized by low cost and high accuracy; it is also not limited by location and space. Stereophotogrammetry can be combined with Pix4D, PhotoScan, and other software to obtain digital elevation model (DEM) data before and after slope erosion to calculate soil erosion and deposition (Guo et al., 2016; Wells et al., 2016). The current study uses stereophotogrammetry to extract the DEM before and after the erosion of an ephemeral gully via a scour experiment. It aims to explore the effect of the upper confluence flow on the erosion–deposition process of an ephemeral gully under the protection of geocell, the change in the development pattern of the ephemeral gully, and the processes of flow and sediment production to provide a scientific basis for the deployment of control measures for ephemeral gully erosion.

2 Materials and methods

2.1 Materials and devices

The experimental device was an adjustable steel trough with a length, width, and height of 3.00 m×2.00 m×0.45 m (Fig. 1). Its slope adjustment range was 0°–30°. To ensure good drainage during the experiment, we set drainage holes with a diameter of 5 mm at 10 cm (length and width) intervals at the bottom of the experimental device. The upper confluence device consisted of a water supply pipe steady-flow flume, and a water tank. The flow rate of the water supply was controlled by a valve in the supply pipe and calibrated before each experiment. The experimental soil was typical cultivated black soil collected at a depth of 0–20 cm from Keshan Farm (48°16′N, 125°20′E), Keshan County, Heilongjiang Province, China. The mechanical components of the soil

were 6.57% slime (<0.002 mm), 67.55% powder (0.002–0.050 mm), and 25.88% grit (>0.050 mm). Soil organic matter content measured using the potassium dichromate external heating method was 72.95 g/kg, and pH (water extraction method, soil to water ratio (1.0:2.5)) was 6.30. The geocell specification was EC200-450. The peel strength of the solder joint was >3000 N, its thickness was 1.3 mm, and its height was 60.0 mm (Fig. 2).

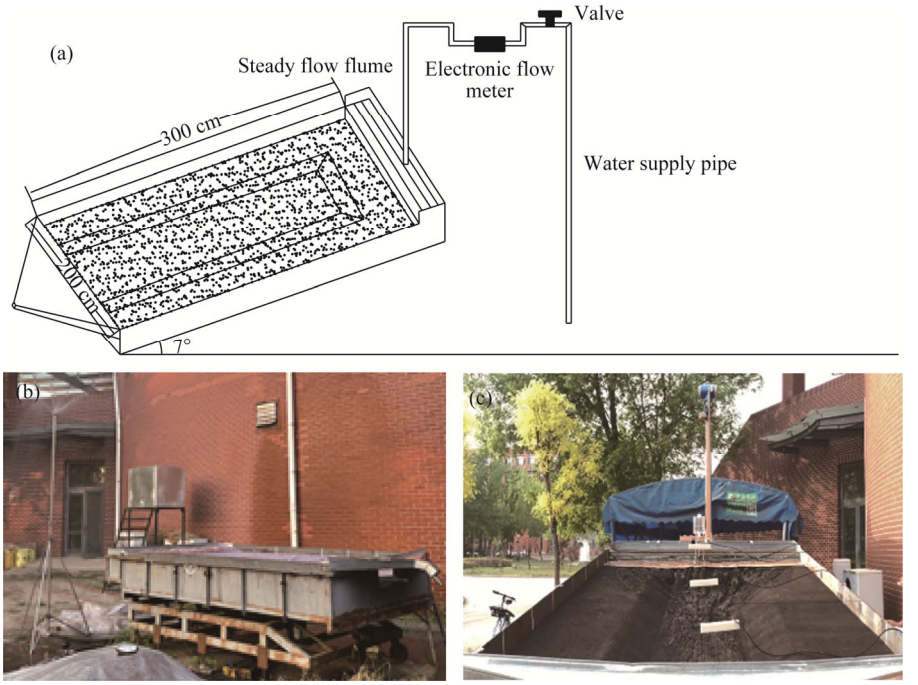

Fig. 1 An illustration of the experimental device. (a), soil flume; (b), pre-rainfall test; (c), flow rate test.

Fig. 2 (a), geocells used in the experiment; (b), geocells exposed from the ground during the experiment.

2.2 Experimental design

The erosion effect of confluence on a sloping farmland is increased during summer and autumn due to the frequent occurrence of high-intensity rainfall in the black soil area of Northeast China, coupled with its special length and gentle slope topography (An et al., 2012; Wen et al., 2015). The high frequency of instantaneous rainfall intensity of 0.71 mm/min was found in the study area (Zhang et al., 1992) with the catchment area of 3 hm^2, the slope length of 200 m, and the observed distance between adjacent ephemeral gullies of 210–270 m (Meng and Li, 2009). Therefore, the flow rates of 0.6, 1.8, 2.4, and 3.0 m^3/h were designed in this study. A slope for the occurrence of gully erosion in the black soil area of Northeast China is 5°–7° (Qin et al., 2014), and because of the influence of microtopography, there is mostly micro-slopes perpendicular to the slope on both sides of the ephemeral gully. Therefore, the experiment designed slope was 7°, and the vertical slope was 3°. An ephemeral gully was scraped out with a scraper 30 cm from the top of the flume. The ephemeral gully was in the middle of the soil flume. The width of the ephemeral gully was 1 m, the slope on both sides was 30°, and the height difference between the gully bottom and the slope on both sides was 7 cm. The cross section of the shallow trench prototype was approximately trapezoidal (Fig. 3). The scrapers used to make the ephemeral gully prototypes were 2 m-long boards (the same width as the experimental trough). To ensure a consistent shape of the ephemeral gully, we used the same scrapers before the experiments. The specific details of the experimental design are shown in Table 1.

Table 1 Details of the experimental design

Flow rate (m^3/h)	Measure	Slope (°)	Experiment repetition
0.6 1.8 2.4 3.0	Control group Geocell	7	2

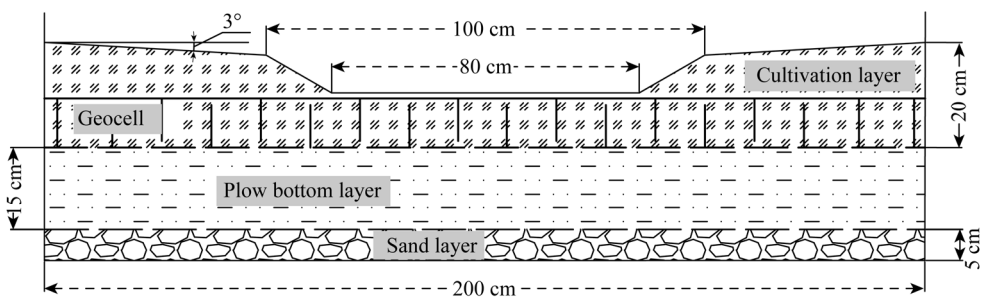

Fig. 3 Experimental soil profile

2.3 Experimental procedure

The experimental soil was treated without grinding to avoid damaging its original structure. The bottom of the experimental flume was covered with gauze before filling with 5 cm of fine sand to ensure good water permeability. Then, another layer of gauze was laid on the sand layer, and the flume was filled with 35 cm of soil. The 35 cm soil layer was divided into a plow bottom layer and a cultivation layer, with the plow bottom layer being 15 cm of loess with a controlled capacity of 1.35 g/cm^3 and the tillage layer being 20 cm of black soil with a controlled capacity of 1.15–1.25 g/cm^3. The geocell was arranged at the junction of the plow bottom layer and the tillage layer, and fixed onto the compacted plow bottom layer with U-shaped nails (the nail length was 15 cm, and the hook was 5 cm). Then, the small cells of the geocell were filled with black soil by using the weight control method, and the weight of the fill was calculated in accordance with the volume and the corresponding moisture content and bulk density. Finally, a rubber hammer was used to compact the soil to the designed height, and a scraper was used to scrape out a shallow ditch shape. Every 5 cm

layer of soil was used for each filling. To ensure that the initial conditions of each experiment were the same, we simulated a pre-rainfall with an intensity of 30 mm/h before every experiment. Once the soil surface was sufficiently full to produce flow, the rainfall was ended, and the trough was covered with a plastic sheet and left for 12 h for the experiment. Soil moisture content varied from 19.3% to 20.5% during the early stages of the experiment. The discharge flow rate was determined before and after the experiment, and the flushing experiment could only be performed when the error between the actual flow and the designed flow was within 5%. Meanwhile, three targets were placed on each side of the soil flume as control points, with each target being 1 m apart. A Canon EOS 70D camera was used to take photographs before and after the experiment. When shooting, we used a fixed focal length to keep the lens and angle consistent (Yang et al., 2010), and the overlap rate of each photo was above 70%–80% (Yang et al., 2018). After the initiation of the experiment, the water overflowed to the steady flow flume to start timing. When runoff reached the collecting port, runoff product time was recorded. After the production of a flow, samples of runoff sediments were collected every 2 min in plastic buckets. Each sample was taken for 20 s, and the whole experiment lasted 45 min. After the experiment, all the received sediment samples were weighed in sequence and poured out of the supernatant. The sediments were transferred to an aluminum box, dried in an oven at 105°C, and weighed.

2.4 Processing of ephemeral gully erosion–deposition data

After the experiment, the photos taken were imported into Agisoft PhotoScan Professional v.1.5.2 software, and preliminary processing was conducted. "Thorn points" were performed on the photos that contained control points, alignment was continuously optimized, and the points were adjusted to make the error less than 1 pixel. Then, the coordinates of the control points were imported to optimize the alignment and eliminate photo distortion. The resolution of the acquired DEM data was 0.3 mm/pix in accordance with the process of constructing a sparse point cloud model, generating a dense point cloud model and DEM output. The DEM of the ephemeral gully before and after scouring was imported into ArcGIS v.10.8, a vector rectangle was drawn, and this vector rectangle was used to crop the DEM so that it covered the entire bottom of the ephemeral gully (Qin et al., 2016, Qin et al., 2018). Then use the "raster calculator" tool to "subtract" the DEM before and after the erosion and obtain the Digital Elevation Change Model (DECM) after the erosion of the ephemeral gully, to show the spatial distribution characteristics of shallow ditch erosion–deposition.

$$\text{DECM}=\text{DEM before scouring}-\text{DEM after scouring}. \quad (1)$$

The reclassification tool was utilized to perform erosion and sedimentation classification processing on the acquired DECM, and the data were exported to excel to obtain the number of pixels that corresponded to the classification.

$$\text{Proportion of erosion (deposition)} = \frac{\text{number of pixels in the erosion (deposition) area}\times\text{resolution}}{\text{total number of pixels in the erosion and deposition area}\times\text{resolution}}. \quad (2)$$

$$\text{Proportion of each erosion-sedimentation classification} = \frac{\text{number of pixels in each erosion (deposition) classification}\times\text{resolution}}{\text{number of pixels in the erosion (deposition) area}\times\text{resolution}}. \quad (3)$$

3 Results

3.1 Effect of geocell on erosion during sediment yield process

Figure 4 showed the sediment yield rate in ephemeral gullies under the flow rates of 0.6, 1.8, 2.4, and 3.0 m^3/h. At different flow rates, the variation trend of sediment yield with time was the same, and they were all in a process of gradually decreasing and tending to be stable. With an increase in confluence flow, the process curve gradually became steeper, the erosion rate gradually increased, and the effect on ephemeral gully erosion was greater. The results showed that the

average rate of erosion sediment yield of the control ephemeral gully increased from 2.22 to 3.30 kg/(m^2·min), while that of the geocell ephemeral gully increased from 1.38 to 2.13 kg/(m^2·min), confirming the anticorrosion effect of geocell measures.

When the flow rate was 0.6 m^3/h, the average rate of sediment yield of the control ephemeral gully was 1.61 times that of the geocell ephemeral gully, and the erosion of the geocell ephemeral gully decreased by 37.84%. When it was 1.8 m^3/h, the sediment yield rate of the geocell ephemeral gully increased by 23.08%. Nevertheless, compared with that of the control ephemeral gully, the average sediment yield rate of the geocell ephemeral gully decreased by 26.09%. When the flow rate increased to 2.4 m^3/h, the average rate of sediment yield of the geocell ephemeral gully further increased to 2.13 kg/(m^2·min), and the erosion decreased by 21.40%. These results showed that the geocell can reduce the erosion of ephemeral gully, and the erosion reduction rate decreased gradually with an increase in flow rate. When the flow rate reached up to 3.0 m^3/h, the average rate yield of sediment was only 2.14 kg/(m^2·min). Compared with the ephemeral gully on bare slopes, the average erosion and sediment yield rate decreased by 35.45%. Under the measures of the geocell, when the flow rate was increased from 0.6 to 2.4 m^3/h, the erosion intensity and total erosion effect of the ephemeral gully increased gradually with an increase in confluence flow, but the erosion reduction ratio of the ephemeral gully decreased gradually. When the flow rate was 3.0 m^3/h, the ephemeral gully erosion reduction rate suddenly increased, and the protective effect was enhanced.

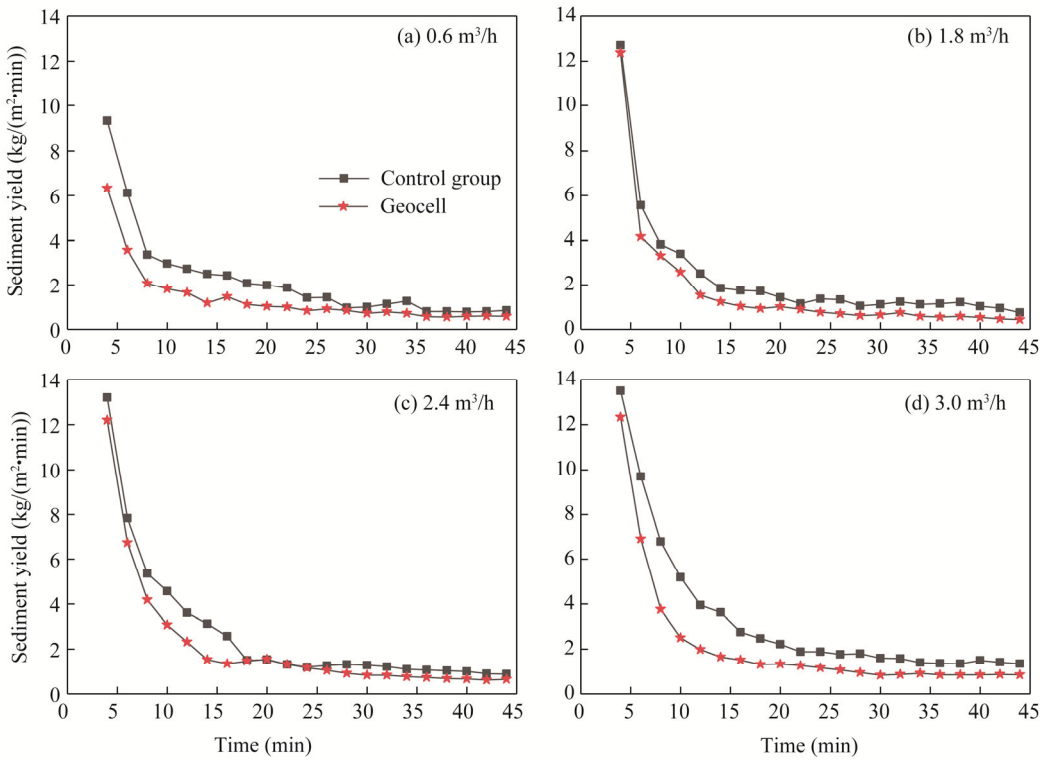

Fig. 4 Sediment yield in the ephemeral gully protected by geocell under different flow rates. (a), 0.6 m^3/h; (b), 1.8 m^3/h; (c), 2.4 m^3/h; (d), 3.0 m^3/h.

3.2 Erosion characteristic of ephemeral gully

Figure 5 showed the erosion patterns of ephemeral gully protected by geocell under different flow rates. At 0.6 m^3/h flow rate (Fig. 5a), the function of geocell has not yet emerged, the surface of the ephemeral gully formed a rill that penetrates the entire slope, and the maximum erosion depth was 10 mm, the deposition thickness was 0–5 mm. When the flow rate was 1.8 m^3/h (Fig. 5b), the

integrity of the water flow was damaged due to the obstruction of the geocell, and some intermittent discontinuous rills were formed on the surface. When the flow rate was 2.4 m^3/h (Fig. 5c), no evident rill was found on the surface of the ephemeral gully, and only serious erosion occurred in the upper part of the ephemeral gully. When the flow rate was 3.0 m^3/h (Fig. 5d), the protective effect of the geocell on the ephemeral gully became more prominent. With the extension of the confluence time, the geocell had obvious energy dissipation and obstruction effects on the runoff, and the carrying capacity of the flow decreased. Many discontinuous dips were formed on the surface, and the most severe erosion still occurred in the upper part of the ephemeral gully. In summary, the effect of the geocell became more evident with an increase in confluence flow. Resistance to the formation of the rill on the surface of the ephemeral gully was stronger, and the anti-erosion effect was better.

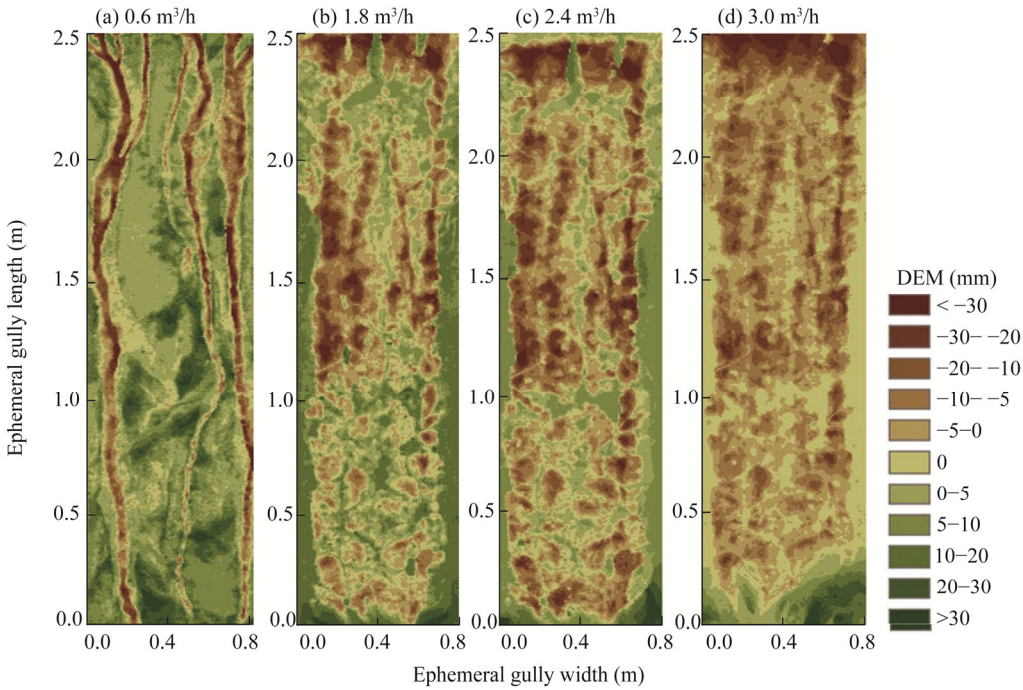

Fig. 5 Erosion pattern of ephemeral gully protected by geocell under different flow rates. (a), 0.6 m^3/h; (b), 1.8 m^3/h; (c), 2.4 m^3/h; (d), 3.0 m^3/h. DEM, digital elevation model.

3.3 Erosion–deposition distribution characteristics

Table 2 and Figure 6 showed that the ephemeral gullies exhibit different degrees of soil erosion and deposition with an increase in confluence flow. When the flow rate was 0.6 m^3/h, the erosion proportion of the ephemeral gully under the geocell was 22.27%, and the deposition proportion was 77.73%. Erosion and deposition thickness is mostly concentrated at 0–5 mm, accounting for 6.75% and 30.10% of the total area, respectively. When the flow rate was 1.8 m^3/h, under the influence of geocell measures, the runoff flowed along the edge of the cell with relatively soft soil, and the area of ephemeral gully erosion had been expanded, so that the proportion of ephemeral gully erosion had increased by 49.56%. Compared with the bare slope, the proportion of erosion still reduced by 40.00%, and the proportion of deposition increased by 1.11 times. Erosion depth was mostly concentrated in 0–5 mm, accounting for 17.54% of the total soil area, while deposition thickness was largely concentrated in 0–5 mm and 10–20 mm, accounting for 18.96% and 18.74% of the total soil area, respectively. When runoff flow increased to 2.4 m^3/h, the erosion rate of the ephemeral gully decreased from 85.03% to 62.33%, the deposition rate increased from 14.97% to 37.67%, and the erosion depth of 0–5 mm accounted for 36.42% of the eroded area of the ephemeral gully. Meanwhile, the deposition thickness values of 0–5 mm and

5–10 mm accounted for 91.40% of the deposition area of the ephemeral gully. When the confluence flow was 3.0 m^3/h, the erosion proportion of the ephemeral gully was 88.75%, and the deposition proportion was 11.25%. These values were similar to the erosion–deposition of the bare slope ephemeral gully; however, the erosion depth was less than 30 mm, and the deposition thickness was larger than 30 mm. No significant increase in the proportion occurred with 1.8 and 2.4 m^3/h flow rates.

Table 2 Soil erosion–deposition proportion of ephemeral gully protected by geocell under different flow rates

Flow rate (m^3/h)	Control group			Geocell			Reduced erosion (%)
	Erosion proportion (%)	Deposition proportion (%)	Average sediment yield rate (kg/(m^2·min))	Erosion proportion (%)	Deposition proportion (%)	Average sediment yield rate (kg/(m^2·min))	
0.6	90.59	9.41	2.22	22.27	77.73	1.38	37.84
1.8	73.58	26.42	2.21	44.15	55.85	1.70	23.08
2.4	85.03	14.97	2.71	62.33	37.67	2.13	21.40
3.0	84.56	15.44	3.30	88.75	11.25	2.14	35.45

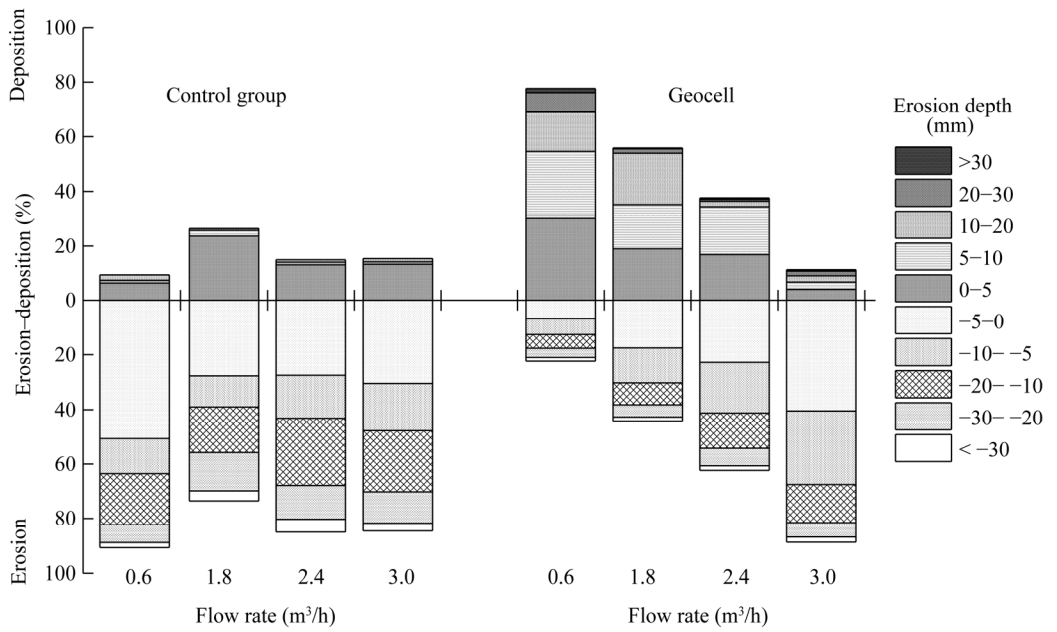

Fig. 6 Erosion–deposition classification of ephemeral gully protected by geocell under different flow rates

4 Discussion

A geocell has a special flexible structure of honeycomb mesh, endowing it with good compressive and shear strengths (Liu et al., 2019). Furthermore, the honeycomb mesh cell structure could separate surface soil at the bottom of the ephemeral gully into independent small pieces. These independent small pieces form an organic whole through the flexible restraint of the geocell, improving overall soil integrity and continuity (Zeng et al., 2017). The high cohesion of the soil in the mesh structure under the action of the binding force provides the soil with a certain stability during concentrated water erosion, and prevents the further development of rills downward, reducing the erosion of ephemeral gullies (Sitharam and Hegde, 2013).

4.1 Sediment production characteristics and erosion patterns of ephemeral gullies under geocell measures

The runoff scouring force was low when the flow rate was 0.6 m^3/h, and erosion depth did not exceed the buried depth of the geocell. Moreover, the rill density was low. With an increase in

experimental flow, the effect of the geocell begins to emerge, surface roughness increases, and the erosion pattern changes accordingly. Initially, given that the geocell was covered with a 1-cm-thick soil layer, the state of scour on the surface of the geocell ephemeral gully was similar to that on the ephemeral gully on bare slopes, and its effect has not yet been realized (Wang et al., 2012). As scouring continues over time, runoff flows down the slope, and erosion occurs in areas where the soil is less resistant to erosion. Runoff also continues to converge in eroded areas, eventually developing further downward and upward and deepening and widening to form fixed rill channels.

After the confluence flow rate increased to 1.8 m^3/h, runoff was subjected to the frictional and binding forces of the exposed slope cells, which change direction and disperse their scouring of the slope surface. The water flow path and integrity were disrupted, and surface soil was spatially protected by the geocell, forming a number of intermittent and discontinuous rills. With the further increase in confluence flow to 2.4 m^3/h, the erosive force of the runoff also increased, water mostly flowed along the edge of the geocell, and a turbulent-like shape gradually appeared (Wang et al., 2012), forming many small erosion pits inside the cell. The water entering the small erosion pits is a swirling current that continues to cut down and deepen the erosion, contributing to the rapid development of each small erosion pit. When confluence flow rate increased to 3.0 m^3/h, the erosion of the upper end of the ephemeral gully intensified, and runoff infiltrated the soil along the edge of the geocell. Soil strength was reduced, and lateral erosion became increasingly evident, creating many deep drop-offs. Geocells obstruct the communication path of runoff, preventing it forming a fixed flow path, and runoff and sand transport channels were cut off, reducing regional sediment connectivity and erosion (Zhang et al., 2011; Zhang and Xie, 2019). Overall, geocell provided a good protective effect at high flow rates.

4.2 Erosion–deposition characteristics of ephemeral gullies under geocell measures

With an increase in confluence flow rate, the erosion proportion of the geocell ephemeral gully increased gradually, while the deposition proportion decreased gradually. At flow rates of 1.8, 2.4, and 3.0 m^3/h, the erosion depths of < -30 mm and >30 mm were not obvious, because the runoff of the ephemeral gully was dispersed by the geocell, expanding the erosion surface of the ephemeral gully. When flow rate increased, the sheer force of the runoff was also enhanced, this soil layer was quickly carried away by runoff, and the amount of sediments was reduced. However, the shear force at this point still does not reach the shear strength of the compartment, and thus some of the kinetic energy of the runoff is consumed (Zeng et al., 2017), and the undercutting ability is significantly weakened. In addition, under the combined actions of the friction force and the lateral restraint force generated by the side walls of the cell on the surface soil, the cohesion of the soil in the geocell is considerably stronger than that of the bare slope soil (Vibhoosha et al., 2021). The ability to prevent runoff erosion is highly improved, and thus, no rill is formed on the surface of the ephemeral gully, but only intermittent erosion, which is also one of the reasons for the reduction in erosion depth. In summary, geocell measures increase the erosion area on the surface of the ephemeral gully but reduce the erosion depth of the ephemeral gully. Intuitively, a geocell changes the erosion mode by adjusting the proportion of ephemeral gully erosion to deposition, converting erosion from rill erosion to sheet erosion. From the DEM images, the most serious erosion under the geocell measures for the four flow intensities designed in this experiment occurs in the upper part of the ephemeral gully, where the upper soil was highly susceptible to denudation. Therefore, in practical applications, the protection of the upper soil must be strengthened in conjunction with other measures to achieve a more comprehensive protection effect.

5 Conclusions

This research explores the effect of geocell measures on sediment yield in ephemeral gully erosion, the evolution of ephemeral gully erosion patterns, and the changes in the

erosion–deposition process under different confluence flow conditions. The major conclusions drawn are as follows. At four confluence flow intensities in the experimental design, the geocells could decrease sediment yield by dissipating energy and influencing the hydrological connectivity path, with a significant increase in the effect on the protection of ephemeral gullies. Geocells significantly influence ephemeral gully erosion patterns. Erosion was most severe in the upper part of the ephemeral gully at all four confluence flow rates. With increasing flow rate, the surface fragmentation of the ephemeral gully became more severe, and the erosion pattern of the ephemeral gully surface changed from continuous rill to intermittent rill, and finally, to an intermittent drop pit. When the flow rate was higher, the role of geocells was more evident. Moreover, the resistance to the formation of rills on the surface of ephemeral gullies was stronger, and the erosion prevention effect was better. The proportion of erosion in the ephemeral gully of the geocell increased gradually while the proportion of deposition decreased gradually as confluence flow rate increased. Meanwhile, the erosion area on the surface of the ephemeral gully increased gradually, while erosion depth decreased gradually. Geocells change the erosion pattern by altering the ephemeral gully erosion–deposition proportion, converting erosion from rill erosion to sheet erosion. The erosion of the upper part of the ephemeral gully under geocell measures was serious and should be combined with other measures to strengthen the upper part of protection when applied in practice.

In this experiment, higher confluence intensity and different geocell distribution patterns were not designed due to the limitations of experimental equipment and other factors. Therefore, investigations on the critical protection flow of geocell measures and the correlation between different spatial distributions and erosion–deposition characteristics were lacking. Future studies should be strengthened to provide a more scientific basis for improving research related to ephemeral gully erosion control and soil conservation in Northeast China.

Acknowledgements

This research was supported by the National Natural Science Foundation, China (41907047), the National Key Research and Development Program of China (2016YFE0202900), and the Natural Science Foundation of Tianjin, China (18JCZDJC39600).

References

An J, Zheng F L, Lu J, et al. 2012. Investigating the role of raindrop impact on hydrodynamic mechanism of soil erosion under simulated rainfall conditions. Soil Science, 177(8): 517–526.

Banerjee L, Chawla S, Kumar Dash S. 2020. Application of geocell reinforced coal mine overburden waste as subballast in railway tracks on weak subgrade. Construction and Building Materials, 265: 120774, doi: 10.1016/j.conbuildmat.2020.120774.

Douglas-Mankin K R, Roy S K, Sheshukov A Y, et al. 2020. A comprehensive review of ephemeral gully erosion models. CATENA, 195: 104901, doi: 10.1016/j.catena.2020.104901.

Guo M H, Shi H J, Zhao J, et al. 2016. Digital close-range photogrammetry for the study of rill development at flume scale. CATENA, 143: 265–274.

Liu H H, Zhang T Y, Liu B Y, et al. 2013. Effects of gully erosion and gully filling on soil depth and crop production in the black soil region, Northeast China. Environmental Earth Sciences, 68(6): 1723–1732.

Liu X B, Li H, Zhang S M, et al. 2019. Gully erosion control practices in Northeast China: A review. Sustainability, 11(18): 5065.

Liu Y, Deng A, Jaksa M. 2019. Failure mechanisms of geocell walls and junctions. Geotextiles and Geomembranes, 47(2): 104–120.

Ma R T, Hu F R, Xu C Y, et al. 2022. Response of soil aggregate stability and splash erosion to different breakdown mechanisms along natural vegetation restoration. CATENA, 208: 105775, doi: 10.1016/j.catena.2021.105775.

Meng L Q, Li Y. 2009. The mechanism of gully development on sloping farmland in black soil area, Northeast China. Journal of Soil and Water Conservation, 23(1): 7–11, 44. (in Chinese)

MWR (Ministry of Water Resources (China)). 2013. Bulletin of First National Water Census for Soil and Water Conservation.

Beijing: China Water & Power Press, 119–235. (in Chinese)

Nouwakpo S K, Huang C H. 2012. A simplified close–range photogrammetric technique for soil erosion assessment. Soil Science Society of America Journal, 76(1): 70–84.

Qin C, Wu H Y, Zheng F L, et al. 2016. Temporal and spatial variation characteristics of rill erosion and hydrodynamic parameters on loessial hillslope. Transactions of the Chinese Society for Agricultural Machinery, 47(8): 146–154, 207. (in Chinese)

Qin C, Zheng F L, Xu X M, et al. 2018. A laboratory study on rill network development and morphological characteristics on loessial hillslope. Journal of Soils and Sediments, 18: 1679–1690.

Qin W, Zuo C Q, Fan J R, et al. 2014. Control measures for gully erosion in black soil areas of Northeast China. China Water Resources, 20(3): 37–41. (in Chinese)

Sitharam T G, Hegde A. 2013. Design and construction of geocell foundation to support the embankment on settled red mud. Geotextiles and Geomembranes, 41: 55–63.

Sutherland R A. 1998. Rolled erosion control systems for hillslope surface protection: a critical review, synthesis, and analysis of available data. I. Background and formative years. Land Degradation & Development, 9(6): 465–486.

Tang C J, Liu Y, Li Z W, et al. 2021. Effectiveness of vegetation cover pattern on regulating soil erosion and runoff generation in red soil environment, southern China. Ecological Indicators, 129: 107956, doi: 10.1016/j.ecolind.2021.107956.

Vibhoosha M P, Bhasi A, Nayak S. 2021. A review on the design, applications and numerical modeling of geocell reinforced soil. Geotechnical and Geological Engineering, 39(6): 4035–4057.

Wang G Y, Liu Y H, Wang X H. 2012. Experimental investigation of hydrodynamic characteristics of overland flow with geocell. Journal of Hydrodynamics, 24(5): 737–743.

Wells R R, Momm H G, Bennett S J, et al. 2016. A measurement method for rill and ephemeral gully erosion assessments. Soil Science Society of America Journal, 80(1): 203–214.

Wen L L, Zheng F L, Shen H O, et al. 2015. Rainfall intensity and inflow rate effects on hillslope soil erosion in the Mollisol region of Northeast China. Nat Hazards, 79: 381–395.

Xiao L G, Lin G Q, Zhao R Q, et al. 2021. Effects of soil conservation measures on wind erosion control in China: A synthesis. Science of the Total Environment, 778: 146308, doi: 10.1016/j.scitotenv.2021.146308.

Xu X M, Zheng F L, Tang Q H, et al. 2022. Upslope sediment-laden flow impacts on ephemeral gully erosion: Evidences from field monitoring and laboratory simulation. CATENA, 209: 105802, doi: 10.1016/j.catena.2021.105802.

Yan C G, Yang X H, Xie Y L, et al. 2005. Experimental research on anti-eroding effect of geocells in loess embankment. Rock and Soil Mechanics, 26(8): 1342–1344, 1348. (in Chinese)

Yang C, Su Z A, Xiong D H, et al. 2018. Application of close-range photogrammetry technology in the study of soil erosion rate on slope farmland. Journal of Soil and Water Conservation, 32(1): 121–127, 134. (in Chinese)

Yang J Y, Qi Y X, Zhao T N, et al. 2010. Measuring soil erosion rate using digital close range photogrammetry and erosion pin techniques. Journal of Beijing Forestry University, 32(3): 90–94. (in Chinese)

Zeng L H, Jiang H, Huang H Q, et al. 2017. Study on erosion resistance of geocell based on artificial rainfall. Yangtze River, 48(10): 9–12. (in Chinese)

Zhang G H, Wang L L, Tang K M, et al. 2011. Effects of sediment size on transport capacity of overland flow on steep slopes. Hydrological Sciences Journal, 56(7): 1289–1299.

Zhang G H, Xie Z F. 2019. Soil surface roughness decay under different topographic conditions. Soil & Tillage Research, 187: 92–101.

Zhang X K, Xu J H, Lu X Q, et al. 1992. A study on the soil loss equation in Heilongjiang Province. Bulletin of Soil and Water Conservation, 12(4): 1–9, 18. (in Chinese)